NUWC-NPT Reprint Report 11,774
5 November 2006

Air-Inflated Fabric Structures

Paul V. Cavallaro
NUWC Division Newport

Ali M. Sadegh
The City College of New York

NEWPORT

Naval Undersea Warfare Center Division
Newport, Rhode Island

Reprint of a chapter in *Marks' Standard Handbook for Mechanical Engineers*, Eleventh Edition, McGraw-Hill, New York, 2006.

TABLE OF CONTENTS

Page

LIST OF ILLUSTRATIONS

AIR-INFLATED FABRIC STRUCTURES: A CHAPTER FOR *MARKS' STANDARD HANDBOOK FOR MECHANICAL ENGINEERS*

INTRODUCTION

Air-inflated fabric structures fall within the category of tensioned structures and provide unique advantages in their use over traditional structures. These advantages include light weight designs, rapid and self-erecting deployment, enhanced mobility, large deployed-to-packaged volume ratios, fail-safe collapse, and possible rigidification.

Most of the research and development pursued in air-inflated structures can be traced to space, military, commercial, marine engineering and recreational applications. Examples include air ships, weather balloons, inflatable antennas and radomes, temporary shelters, pneumatic muscles and actuators, inflatable boats, temporary bridging, and energy absorbers such as automotive air bags. However, the advent of today's high performance fibers combined with continuous textile manufacturing processes has produced an emerging interest in air-inflated structures. Air-inflated structures can be designed as viable alternatives to conventional structures.

Because these structures combine both the textile and structural engineering disciplines, the structural designer should become familiar with the terminology used in textile materials and their manufacturing processes. A glossary is provided in reference [1].

DESCRIPTION

Air-inflated fabric structures are constructed of lightweight fabric skins that enclose a volume of pressurized air. The fabric is typically formed in a variety of textile architectures including those shown in figure (1). Each architecture has its own design, manufacturing, tooling and cost implications. Structurally, these architectures will behave differently when subjected to loads.

The plain-weave architecture provides orthogonal yarn placement resulting in extensional stiffness along the two yarn axes; however, it lacks shear stiffness for off-axis loads. While the braided architecture provides the fabric with shear stiffness due to the non-orthogonality of the yarns, it lacks extensional stiffness. The angle between the braid axis and the yarns, θ, is referred to as the braid angle or bias angle. Both the triaxial braid and axial strap-reinforced braid architectures behave similarly in that they afford the fabric with extensional and shear stiffnesses.

The air pressure develops a biaxial pre-tensioning stress throughout the fabric. This pre-tensioning stress enables the structure to generate its intended shape, provides stiffness to resist deflections and affords stability against collapse from external loads. Fabric materials can often be idealized as tension-only materials for design purposes, that is, their in-plane compressive moduli and bending moduli are considered negligible.

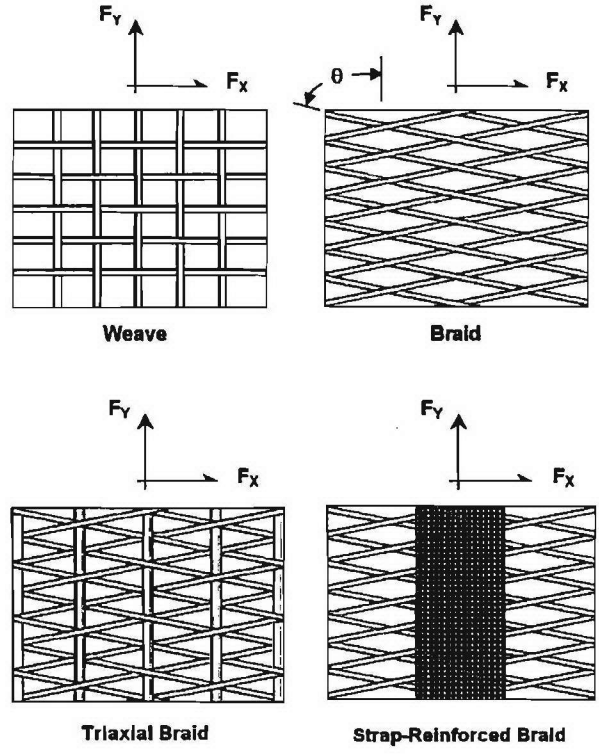

Figure 1. Various fabric architectures used in air-inflated fabric structures.

Stiffness of the structure is primarily a function of the inflation pressure. As the inflation pressure increases, the pre-tensioning stresses throughout the fabric increase and, in turn, stiffen the structure. Once external loads are applied, stresses from these loads superimpose with the pre-tensioning stresses in the fabric. As a result, a complete redistribution of stress occurs. This stress redistribution balances the loads and maintains the structure in a state of static equilibrium. Depending upon the type of air-inflated fabric structure (i.e.; beam, arch, etc.) and applied loads (i.e.; tension, compression, shear, bending, torsion, etc.), the redistribution of stresses can either increase or decrease the net tension stresses in the fabric skin. However, stability of the structure is only ensured when no regions of the fabric experience a net loss in tensile stress. Otherwise, if the stresses from applied loads begin to relax the pre-tensioning stress (i.e.; the tension approaches zero), the onset of wrinkling is said to have occurred within the structure. Wrinkling decreases the structure's load carrying capability and upon further loading, eventual buckling or collapse will result.

There are two significant and unique characteristics that air-inflated fabric structures provide over conventional structures. First, upon an overload condition, a collapse of an air-inflated structure does not necessarily damage the fabric membrane. When the overload condition is removed, the air-inflated fabric structure simply restores itself to its design load configuration. Second, since wrinkling can be visually detected, it can serve as a warning indicator prior to collapse.

FIBER MATERIALS AND YARN CONSTRUCTIONS

Proper selection of fiber materials and yarn constructions are important factors that must be considered in the design of air-inflated fabric structures. Both should be optimized together to achieve the desired performance characteristics at the fabric and structural levels.

Many of today's air-inflated fabric structures use yarns constructed of high performance continuous fibers such as Vectran® (thermoplastic liquid crystal polymer) PEN® (polyethylene naphthalate), DSP® (dimensionally stable polyester), and others. These fibers provide improved structural performance (high strength, low elongation, fatigue, flex-fold, cyclic loadings, creep, etc.) and enhanced environmental resistance (ultraviolet rays, heat, humidity, moisture, abrasion, chemicals, etc). Other fibers used in air-inflated fabric structures include Kevlar®, Dacron®, nylon, Spectra® and polyester. Hearle[2] provides additional information on fiber materials and their mechanical properties.

Yarns are constructed from fibers that may be aligned unidirectionally or arranged in a number of twisted bundles. Twist is used to improve the handling susceptibility of the yarns by grouping the fibers together especially during textile processing. Twist, which is measured in turns per unit yarn length, affects the yarn tensile properties. For discontinuous or staple fiber yarns, twist can increase the yarn breaking strength because the internal forces at the ends of a fiber can transfer to neighboring fibers via inter-fiber shear forces. However, twist in continuous fiber yarns can reduce the yarn breaking strength as observed by Hearle[3]. Therefore, a minimal twist is recommended for providing adequate handling protection to continuous fiber yarns.

Hearle[3] experimentally investigated the effects of twist on the tensile behavior of several continuous fiber yarns. His results showed that yarn tenacity (defined as tensile strength measured in grams-force per denier or grams-force per tex) decreased with increasing twist for 3 prescribed yarn tensions used during twist formation. In general, the yarn modulus decreased with increasing twist, yarn elongation at break increased with increasing twist, and yarn elongation decreased with increasing yarn tension. A difference in the load-extension behavior of twisted and non-twisted yarns is that a twisted yarn when subjected to tension will undergo compaction of its cross section through migration of its fibers and develop greater inter-fiber frictional forces than a non-twisted yarn. Like fabrics, the structural performance of yarns can be tailored by changes in their architecture and processing.

Once the yarns are processed into the fabric (i.e.; by weaving, braiding, etc.), it is recommended that tensile tests be performed on sample yarns removed from the fabric. This will allow the "as-processed" yarn properties to be compared to the design requirements. For example, the "as-woven" tensile properties of continuous-fiber, non-twisted yarns removed from a plain-woven fabric air beam were measured[4] using an Instron machine configured with textile grips as shown in figure (2). The cross sectional areas of the yarns were computed based on fiber diameter and quantity. The tests revealed that the average breaking stress of the weft yarns was nearly 20% less than that of the warp yarns. The reduction in breaking stress of the weft yarns was due to fiber damage caused by the use of higher tensions in these yarns during weaving.

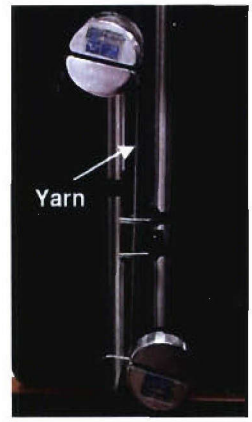

Figure 2. Yarn tensile testing using Instron® textile grips.

EFFECTS OF FABRIC CONSTRUCTION ON STRUCTURAL BEHAVIOR

Fabric materials are constructed from yarns that cross over and under each other in a repetitive, undulating pattern. The undulations shown in figure (3) are referred to as crimp, which is based on Pierce's geometric fabric model[5] .

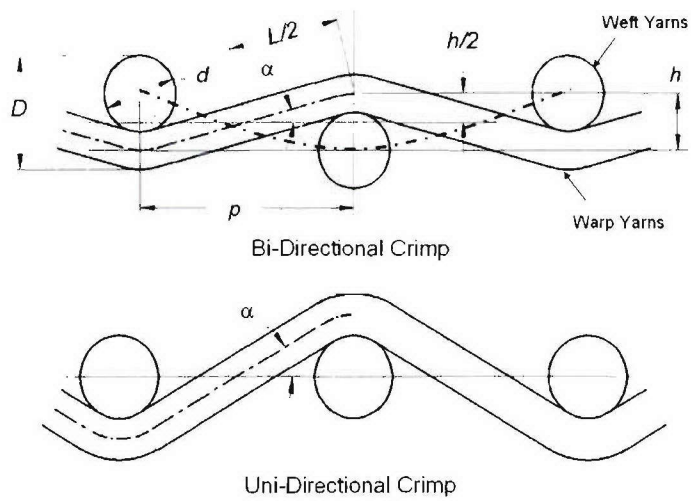

Figure 3. Examples of Pierce's geometric model for plain-woven fabrics with bi-directional and uni-directional crimp.

Pierce's geometric model relates these parameters as they are coupled among yarn families. The crimp height, h, is related to the crimp angle, α, and yarn length, L, as measured between yarns, and the sum of yarn diameters at the cross over points by the following equations described by Grosberg [3]:

$$\begin{aligned} p &= (L - D\alpha)\cos\alpha + D\sin\alpha \\ h &= (L - D\alpha)\sin\alpha + D(L - \cos\alpha) \\ D &= h_1 + h_2 . \end{aligned} \tag{1}$$

These equations were based on idealized geometry and assumptions such as restricting the yarns to circular cross sections and no consideration of force or stiffness effects.

Plain-woven and braided fabrics behave differently under load because their yarn families are aligned at different angles. Plain-woven fabrics utilize a nearly orthogonal yarn placement of warp and weft (or fill) yarns. By general textile definitions, warp yarns are identified as those yarns running parallel to the selvage and are virtually unlimited in their length. Weft yarns are at right angles to the selvage and are limited in length by the width of the weaving equipment. On the other hand, braided fabrics have a $+\theta/-\theta$ yarn placement, where θ is commonly referred to as the bias angle, with respect to the braid axis.

The biaxial stress-strain behavior of plain-woven fabrics is initially dominated by crimp interchange rather than yarn elasticity. Because the factors of safety used in air-inflated fabric structures are typically within the range of 4-6, the operating stresses are designed to be low with respect to fabric strength. Therefore, the structural performance of fabrics must address the influences of crimp interchange. The relative yarn motions (slip and rotation) affect the stiffness properties. The crimp ratio, which is denoted as C, is defined as the waviness of the yarns and is obtained by measuring the length of a yarn in its fabric state, L_{fabric}, and the length of that same yarn after it has been extracted from the fabric, L_{yarn}, and straightened out according to equation (2).

$$C = \frac{L_{yarn} - L_{fabric}}{L_{fabric}}. \tag{2}$$

The following equation described by Grosberg relates the crimp height to C.

$$\frac{h}{p} = \frac{4}{3}\left(\frac{L}{p} - 1\right)^{\frac{1}{2}} \equiv \frac{4}{3} C^{\frac{1}{2}}. \tag{3}$$

Consider a plain-woven fabric subject to a tensile load along the direction of one yarn family. The loaded yarns will attempt to straighten, decrease their crimp heights and elongate their effective lengths. However, the yarns of the crossing family are forced to increase their crimp heights resulting in contractions of their effective lengths. The effect associated with changes in crimp is referred to as crimp interchange and is similar to the Poisson's effect exhibited in metals. Crimp interchange is a coupling effect exhibited between yarn families. When a fabric is loaded in tension, the crimp contents become mutually altered as the yarns attempt to straighten. In tests of plain-woven fabrics along the direction of a given yarn family, crimp interchange can be easily observed by reducing the width of the specimen. Crimp interchange is a source of nonlinear load-extension behavior for fabrics.

Backer[3] describes a limiting phenomenon to crimp interchange. As the biaxial tensile loads continually increase for a given loading ratio, a configuration results in which yarn kinematics (i.e.; slip at the cross over points) cease and the spacing between yarns converge to

minimum values. This configuration is referred to as the extensional jamming point, which can prevent a family of yarns from straightening and thereby not achieve its full strength. Crimp interchange depends upon the ratio of initial crimp between yarn axes and the ratio of stress between yarn axes rather than the levels of stress. Crimp interchange introduces significant nonlinear effects in the mechanical response of the fabric.

Now consider the plain-woven fabric subjected to shearing by applying a uniaxial load at ±45 degrees to either yarn family. The yarn families will rotate at the crossover points with respect to each other and become increasingly skewed as the angle between the yarns changes. The change in angle is referred to as the shear angle. At larger shear angles, the available space between yarn families decreases and rotational jamming (locking) of the yarn families occur. This phenomenon is known as shear-jamming and the angle at which the yarn families become jammed is referred to as the shear-jamming angle. The shear-jamming angle decreases with increasing yarn density ratio and can be estimated from Pierce's geometric fabric model or obtained experimentally with various trellising or biaxial test fixtures. Continued loading beyond the onset of shear-jamming will produce shear wrinkles leading to localized out-of-plane deformations.

It is important to determine the extension- and shear-jamming points for both fabric manufacturing and structural stiffness concerns. In general, jamming is related to the maximum number of weft yarns that can be woven into a fabric for a given warp yarn size and spacing.

OPERATION

Today's air-inflated fabric structures can be operated at various pressure levels depending upon fabric architecture, service loads and ambient temperatures. Woven structures are generally designed to operate at pressures up to 20 psi while triaxial braided and axial strap-reinforced braided structures are generally capable of higher inflation pressures. Blowers, which may be used for inflation pressures up to 3 psi, provide a high volumetric air flow rate. However, air compressor systems will be required for higher inflation pressures. Air compressors are available in single and dual stage configurations. The single stage air compressor delivers a high-pressure capability but at a low volumetric air flow rate. The volumetric flow rate is measured in standard cubic feet per minute (scfm). Dual stage air compressors are designed to provide an initial high volumetric air flow rate at low pressures in the first stage and can be followed by a low volumetric air flow rate at high pressure. When a dual stage air compressor is used, the first stage is most beneficial to erecting the fabric structure. At this time, no appreciable resistance to the design loads is available. However, the second stage mode of the compressor is used to fully inflate the fabric structure to its proper operating pressure so that the design loads can be supported. Because the dual stage compressor can achieve the desired inflation pressure much more rapidly than the single stage compressor, it is more appropriate for those applications in which the need for rapid deployment justifies the additional cost.

INFLATION AND PRESSURE RELIEF VALVES

Valves designed for use in air-inflated fabric structures must consider several criteria including locations, orifice size, pressure relief controls and potential strength degradation in the surrounding fabric regions. Ideally, valves should be positioned in structural elements that interface with the fabric and bladder such as metal clamps, discs or end plates at the end termination zones of the structure. This avoids the need for cutting additional penetration holes through the fabric or repositioning the yarns to accommodate holes for valve placement, thus preventing stress concentrations. When fibers must be removed to accommodate insertion of valves, fabric reinforcement layers should be bonded and stitched to the main fabric in the surrounding region. The valves should be readily accessible for user access but should not jeopardize the integrity of the fabric when the structure is subjected to handling events (such as drops, impacts, etc.). Valve locations should be further optimized to mitigate the effects of interference with other objects when the structure is deployed or stowed.

A variety of pneumatic valve designs including threaded valves, quick connect-disconnect valves, check valves (one-way, two-way), pressure relief valves, etc. are readily available. The use of pressure relief valves is recommended to avoid accidental overpressures and pressure increases due to changes in ambient temperatures. Valves can also be configured to manifold inflation lines in air inflated structures containing multiple pressure chambers. This also provides capabilities for self-erecting and controlled deployments by sequencing the inflation timing of multiple chambers. Sizing of the valve orifices should be matched to provide the optimal inflation and deflation times for the air volumes and operating pressures required by the structure.

CONTINUOUS MANUFACTURING AND SEAMLESS FABRICS

Prior to continuous circular weaving and braiding processes in use today, air-inflated fabric structures were constructed using adhesively bonded, piece-cut manufacturing methods. These methods were limited to relatively low pressures because of fabric failures and air leakage through the seams. Continuous weaving and braiding processes can eliminate or minimize the number of seams resulting in improved reliability, increased pressure capacities and greater structural load carrying capability. However, when seams can not be avoided, the seam construction should be designed in such a way that failure of the surrounding fabric occurs rather than the seam. For the safe and reliable use of air-inflated fabric structures, sufficient factors of safety against burst and seam failures must be provided. To guard against burst, for example, a minimum factor of safety of 4-6 is used on yarn strength for each yarn family.

Like traditional composite materials, fabrics can be tailored to meet specific structural performance requirements. Fiber placement can be optimized for air-inflated fabric structures by varying the denier of the yarns (defined as the mass in grams of a 9,000 meter length yarn) and yarn counts along the each direction. For instance, consider a pressurized fabric cylinder. The ratio of hoop stress per unit length to axial stress per unit circumference is 2:1. One can ensure equal factors of safety against yarn burst in the weft (hoop) and warp (longitudinal) yarns by weaving twice as many weft yarns per unit length of air beam than the number of warp yarns per

unit circumference. Alternatively, the same can be accomplished by doubling the denier of the weft yarns in comparison to the denier of the warp yarns.

IMPROVED DAMAGE TOLERANCE METHODS

Assorted methods are used to enhance the reliability of air-inflated fabric structures against various damage mechanisms. Resistance to punctures, impacts, tears and abrasion can be improved by using high-density weaves, rip-stop fabrics and coatings. High-density weaves are less susceptible to penetrations and provide greater coverage protection for bladders. Rip-stop fabrics have periodic inclusions of high tenacity yarns woven in a cellular arrangement used to prevent fractures of the basic yarns from propagating across cells as shown in figure (4). (The breaking strength of a yarn is referred to as tenacity which is defined in units of grams-force per denier. Denier is a mass per unit length measure expressed as the mass in grams of a 9,000 meter long yarn.) The high tenacity yarns contain fractures of the basic yarns and prevent fractures from propagating across cells.

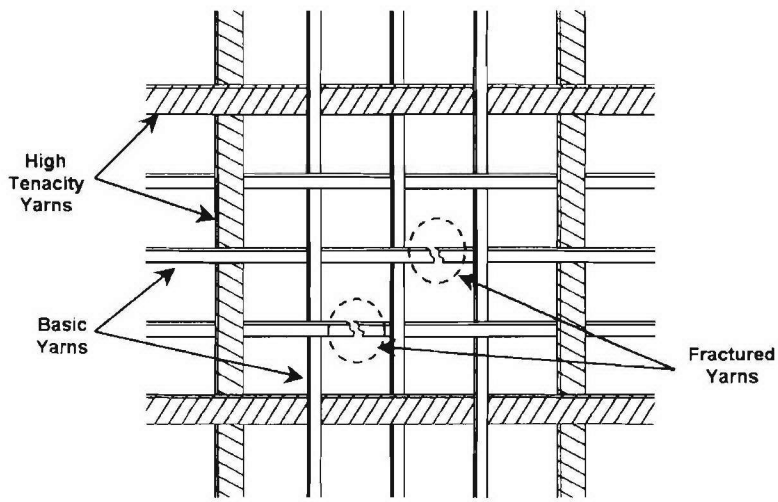

Figure 4. Rip-stop fabric architecture.

Additionally, coatings protect the fabric against environmental exposure to ultraviolet rays, moisture, fire, chemicals, etc. Coating such as urethane, PVC (polyvinyl chloride), neoprene, EPDM (ethylene propylene diene monomer) are commonly used. Additives such as Hypalon further enhance a coating's resistance to ultraviolet light and abrasion. Coatings can be applied in two stages. First, coating the yarns prior to forming the fabric by a liquid bath immersion provides the best treatment to the fibers. Second, coatings can be applied by spraying, painting or laminating directly to the fabric after forming. This stage coats the yarns and bridges the gaps formed between adjacent yarns. The maximum protection is achieved when both stages are utilized. While protective coatings have been shown to increase the stiffness of the fabric by restricting relative yarn motions, they remain flexible enough to not adversely impact the stowing and packaging operations of the structure. Additional information on coating materials and processes is provided by Fung[6].

RIGIDIFICATION

Air-inflated fabric structures can be rigidified by coating the fabric with resins such as thermoplastics, thermosets, shape memory polymers, etc. Prior to inflation, these particular coatings are applied to the fabric and remain initially uncured, thus acting as flexible coatings. After the structure is inflated and properly erected, a phase change is triggered in the coating by a controlled chemical reaction (curing process) activated by exposure to elevated temperature, ultraviolet light, pressure, diffusion, etc. Once the phase change is fully developed, the coatings bind the yarns together, stiffen the fabric in tension, compression and shear, and behave similar to a matrix material found in traditional fiber-reinforced composites. The air–inflated fabric structure is now rigidified and no longer requires the inflation pressure to maintain its shape and stiffness. Depending upon the coating used, the transition process may be permanent or reversible (except where thermoset plastics are used). Reversible rigidification is especially suited for those applications requiring multiple long-term deployments.

The performance of the rigidified fabric structure can be assessed using laminated shell theory (LST) as described by Jones[7]. Unlike the inflated version of the structure, the elastic and shear moduli of the rigidified structure are based on the constituent properties of the fibers and cured coating. As such, the elastic and shear moduli can be readily estimated by using LST. However, the rigidified structure may have different failure modes than its pressurized counterpart. The designer must guard against new failure modes including localized shell buckling and compression rather than wrinkling.

Rigidification is of particular interest for space structures because of restrictions on payload weights and stowage volumes. Cadogan et al[8,9] have pursued the use of shape memory composites for rigidizing deployable space frames.

AIR BEAMS

Fabric air beams are examples of air-inflated structural elements that are capable of supporting a variety of loads similar to conventional beams. To date, seamless air beams have been constructed using continuous manufacturing methods that have produced diameters ranging up to 42 inches. They are constructed of an outer fabric skin that contains an internally sealed film or bladder made of an impermeable elastomer-like material. The bladder contains the air, prevents leakage and transfers the pressure to the fabric. The air beam has a cylindrical cross section and its length can be configured to a straight or curved shape such as an arch. The ends are closed using a variety of end termination methods consisting of bonding, stitching, mechanical clamps, etc. depending upon the inflation pressure and loading requirements. Clamping methods are available to permit disassembly, repair and replacement of the bladder and fabric layers.

Once an air beam is sufficiently pressurized, the fabric becomes pre-tensioned and provides the air beam with a plurality of stiffnesses including axial, bending, shear, and torsion. Upon inflation, the ratio of hoop (cylindrical) stress per unit length of beam to the longitudinal stress per unit circumference is 2:1 as shown in figure (5).

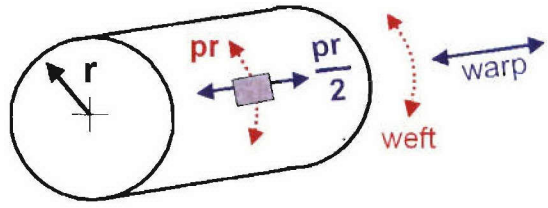

Weft yarn tension per unit length of cylinder = pr

Warp yarn tension per unit circumference = pr/2

$$\text{Yarn density ratio (YDR)} = \frac{\text{\# weft yarns per unit length of cylinder}}{\text{\# warp yarns per unit circumference}}$$

Figure 5. Yarn tensions in a plain-woven pressurized fabric cylinder and definition of yarn density ratio.

In the context of plain-woven air beams, the warp yarns are aligned parallel to the longitudinal axis of the air beam and resist axial and bending loads. The weft yarns spiral through the weave and are located at nearly 90° to the warp axis, thus lying along the hoop direction of the air beam. Weft yarns provide stability against collapse by maintaining the circular cross section of the air beam.

For braided air beams, the braid axis is aligned with the longitudinal axis of the air beam. If the ends of a braided air beam are unconstrained from moving in the longitudinal direction, the fibers will exhibit a scissoring effect causing the length of the beam to expand or shorten with pressure depending upon the selection of θ. Eventually, the braided yarns will achieve a maximum rotation and the fabric will become fully jammed. This phenomenon can be easily demonstrated with the well-known Chinese finger trap toy. Unlike plain-woven fabric structures, the bias angle of braided fabric structures can be controlled to allow expansion or contraction of the structure when inflated. For an unconstrained braided air beam to resist axial tension, longitudinal reinforcements such as distributed axial yarns (i.e.; triaxial braid) or axial straps, webbing, belts, etc. must bonded on at multiple locations around the circumference. Various design methods for constructing axial-reinforced braided fabric air beams were developed by Brown[10] and Brown and Sharpless[11,12].

The bending stiffness, EI, for metal beams is written as the product of elastic modulus, E, and area moment of inertia, I, and has units of (force x distance^2). However, in air inflated fabric structures, the fabric elastic modulus, E_f, is commonly denoted in units of (force per unit length) and therefore, $E_f I$ is denoted in units of (force x distance^3). Likewise, fabric strengths are denoted in units of (force per unit length).

Now, consider the air beam subjected to transverse loads. Upon loading, the pre-tension stresses and the bending stresses will algebraically add. That is, the compressive bending stresses will subtract (relax) from the pre-tension on the compressive surface of the air beam while the tensile bending stresses will add to the pre-tension along the tensile surface as shown in figure (6). The instant at which any point along the length of the air beam develops a net zero longitudinal tensile stress, the structure is said to have reached the onset of wrinkling. The corresponding bending moment is referred to as the wrinkling moment, M_w. Prior to wrinkling, the moment-curvature relationship is expectedly linear in the absence of both material nonlinearities and notable changes in air pressure and volume. A stress balance analysis based on strength of materials equations can generally be used to compute M_w. Such a stress balance analysis was used to show the variation of warp yarn tensions for a 2" diameter plain-woven air beam subjected to 4-point bending loads as depicted in figure (7). Once wrinkling has occurred, the air beam moment-curvature relation behaves nonlinearly because with further loading, the cross section loses bending stiffness, the neutral axis displaces away from the centroidal axis of the cross section and eventual collapse occurs. The spread of wrinkling around the circumference is similar to the flow of plasticity in metal beams subjected to bending. Loading beyond the wrinkling onset will result in an increase of pressure due to loss of volume and the work done on the air will affect the post-wrinkled bending stiffness. Thus, the post-wrinkled response becomes nonlinear. The superposition of the pressure and bending-induced forces is shown for each architecture in figure (8).

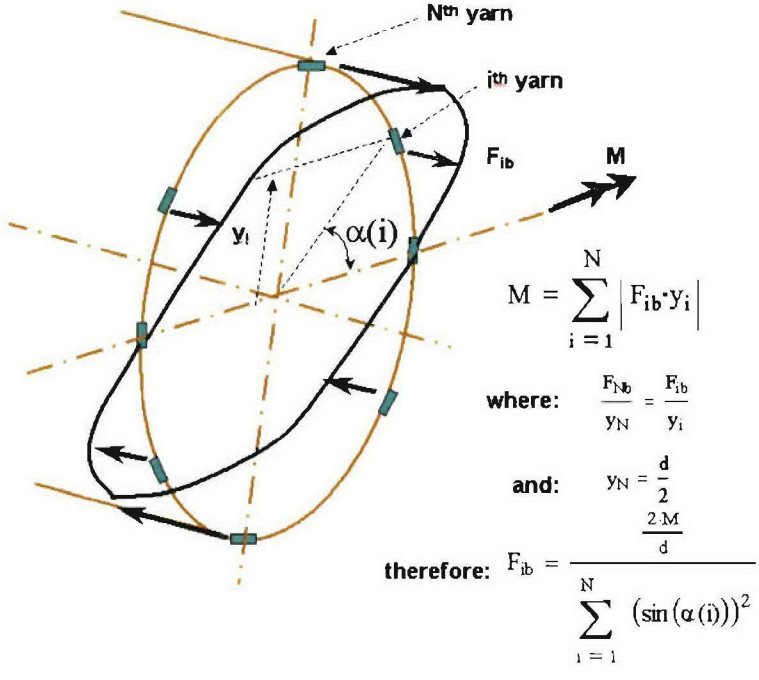

Figure 6. Idealized distribution of warp yarn forces due to bending of a plain-woven fabric air beam.

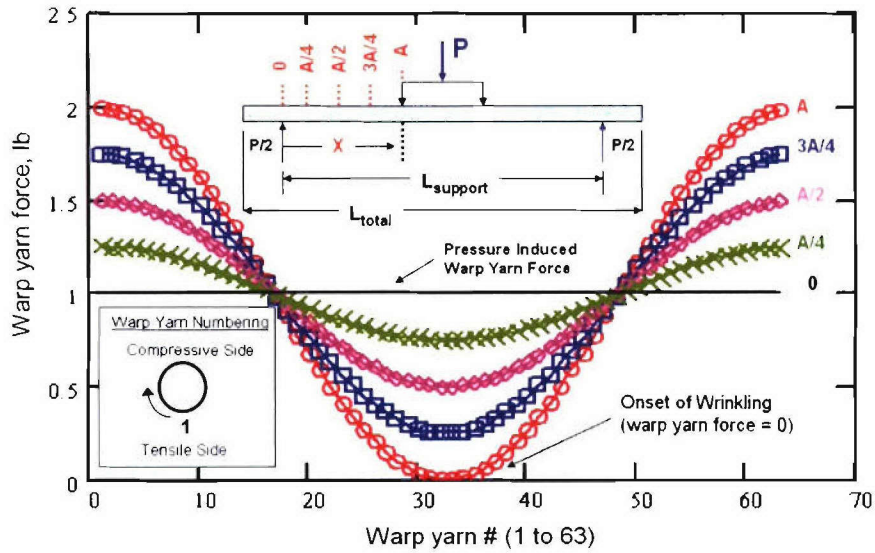

2" dia, 63 Warp yarns, L_{total} = 96", $L_{support}$ = 44.375", A = 14.625",
Pressure = 20 psi, P_{wr} = 4.3 lbs, $Moment_{wr}$ = 31.44 in-lbs

Figure 7. Combined pressure and bending induced forces in warp yarns at various distances along a plain-woven air beam based on a simple stress balance analysis.

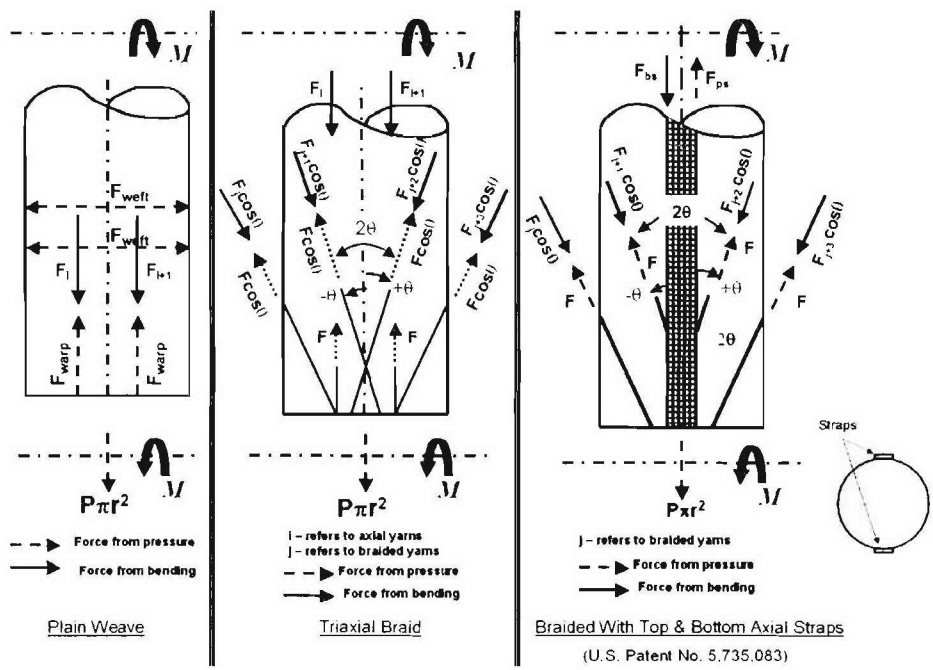

Figure 8. Superposition of pressure and bending induced yarn forces in plain-woven air beam, a triaxial braided air beam and a dual axial strap-reinforced braided air beam.

Consider now a plain-woven air beam subjected to inflation pressure P. The force in the warp yarns, F_{WARP}, is shown in equation (4) as simply the pressure times the cross sectional area divided by the number of warp yarns, N_{WARPS}. The force in the weft yarns, F_{WEFT}, was idealized by the assumption of orthogonal yarn placement and is shown in equation (5). The wrinkling moment, M_W, for a woven air beam was derived from a simple force balance of the pressure and bending-induced yarn forces and is shown in equation (6).

$$F_{WARP} = P \pi r^2 / N_{WARPS} \tag{4}$$

$$F_{WEFT} = P \pi r L / N_{WEFTS} \tag{5}$$

$$M_W = \frac{P \pi r^3}{2} \tag{6}$$

Note that M_W is independent of the fabric material properties.

The global flexure response of plain-woven air beams was experimentally investigated for use in inflatable military shelters[13,14]. The air beams were constructed of non-twisted yarns and were inflated to various operating pressures. Operating pressures were considered to be safe when the resulting yarn tensions did not exceed 30% of their breaking strength. The experimental set up is shown in figure (9). A plot of the experimental load versus deflection is shown in figure (10) which exhibited a significant influence on inflation pressure.

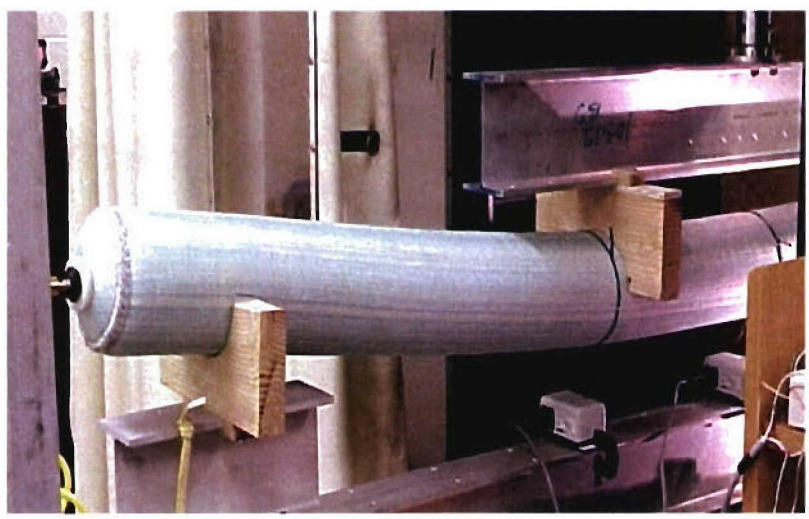

Figure 9. 4-Point flexure test on a 6 inch diameter plain-woven air beam constructed of 3,000-denier, 2:1 YDR Vectran fabric.

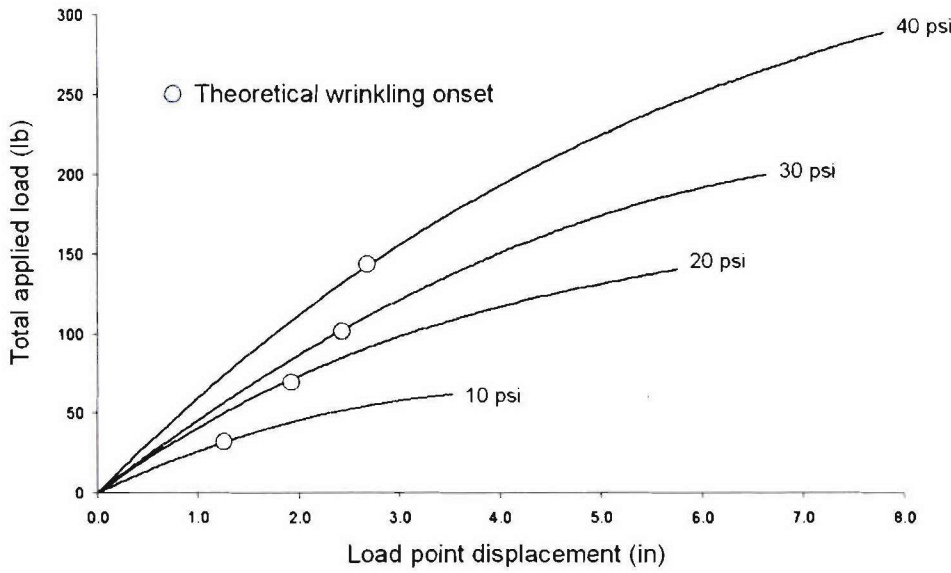

Figure 10. Experimental load vs. deflection plot for an uncoated 6-inch diameter air beam constructed of 3,000-denier non-twisted Vectran yarns in a plain-woven 2:1 Yarn Density Ratio fabric using a 37-inch span between load points and an 85-inch span between support points.

A second series of 4-point bending tests[4] was conducted on a 2-inch diameter, uncoated plain-woven Vectran air beam to measure the midspan deflections as a function of inflation pressures ranging from 10-100 psi. The load versus mid-span deflection curves are shown in figure (11).

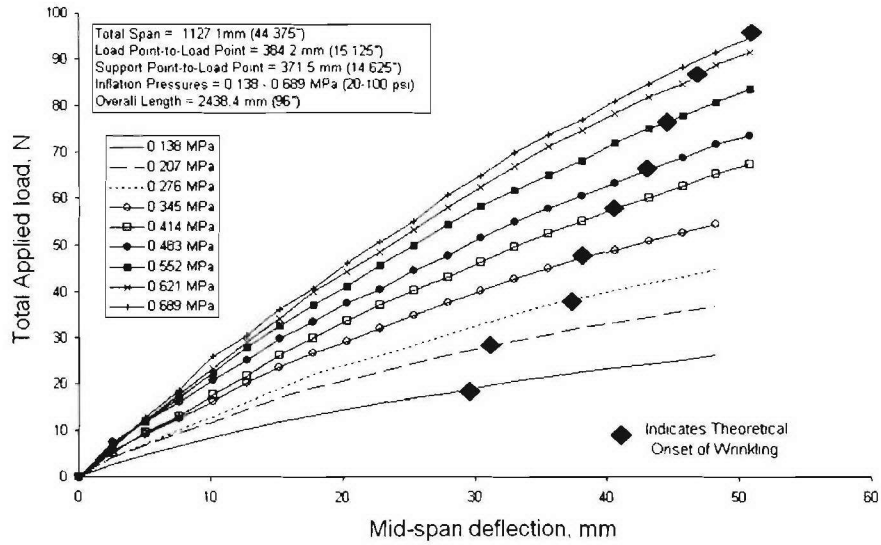

Figure 11. Plot of total load vs. mid-span deflection for a 2-inch diameter plain-woven air beam constructed of 1,500-denier, 2:1 YDR Vectran fabric.

In a third series of tests[4], the flexure behavior of uncoated plain-woven Vectran and PEN air beams were compared for 2 pressures using a constant load point displacement rate. Both air beams had identical crimp in the warp and weft yarns, yarn density ratios (YDR), denier, diameter and length. (The yarn density ratio is defined as the number of weft (hoop) yarns per unit beam length divided by the number of warp (longitudinal) yarns per unit circumference.) The graph of figure (12) shows the total applied load versus the mid-span deflection responses.

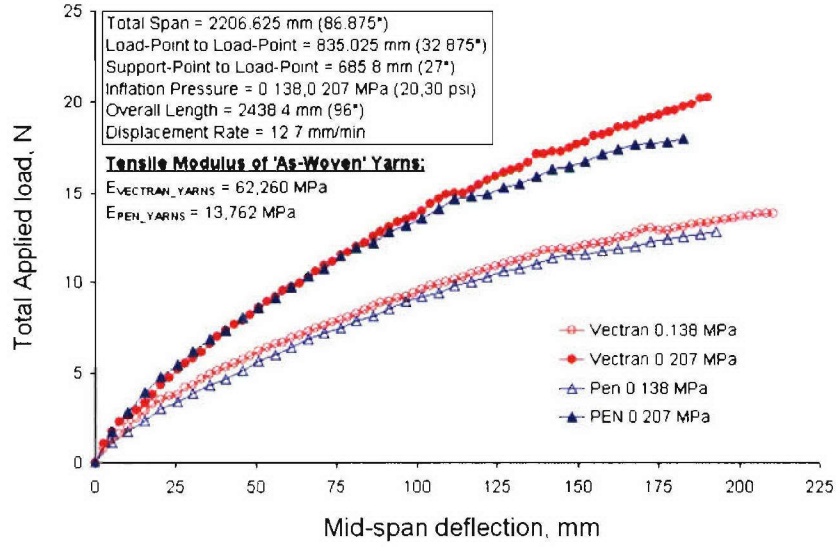

Figure 12. Comparison of 2-inch diameter Vectran and PEN plain-woven air beams subjected to 4-point bending tests at various load point displacement rates.

Although the ratio of the as-woven elastic moduli of the Vectran and PEN yarns obtained through "as-woven" yarn tensile tests was 4.7-to-1.0, there were minimal differences in deflections of these air beams at the inflation pressures used. It was observed that the global bending behavior of the air beams was: (1) invariant with E_{yarn} for the range of inflation pressures considered, (2) dominated by the kinematics of crimp interchange and (3) subjected to considerable transverse shearing deformations. The effects of crimp interchange and shearing deformations precluded the use of traditional strength-of-materials design methods for plain-woven fabric air beams.

DROP-STITCHED FABRICS

Drop-stitch technology, originally pursued by the aerospace industry, extends the shapes that air-inflated fabric structures can achieve to include flat and curved panels with moderate to large aspect ratios and variable thickness. Drop-stitched fabric construction consists of external skins laminated to a pair of intermediate woven fabric layers separated by a length of perpendicularly aligned fibers (Fig. 13). During the weaving process of the intermediate layers, fibers are "dropped" between these layers. Upon inflation, the intermediate layers separate forming a panel of thickness controlled by the drop-stitched fiber lengths. Flatness of the inflated panel can be achieved with a sufficient distribution of drop-stitching. The external skins

can be membranes or coated fabrics which serve as impermeable barriers to prevent air leakage, thus eliminating the need for a separate bladder. Air-inflated structures incorporating drop-stitched fabrics include floors for inflatable boats, energy absorbing walls, temporary barriers, lightweight foundation forms, and a variety of recreational products.

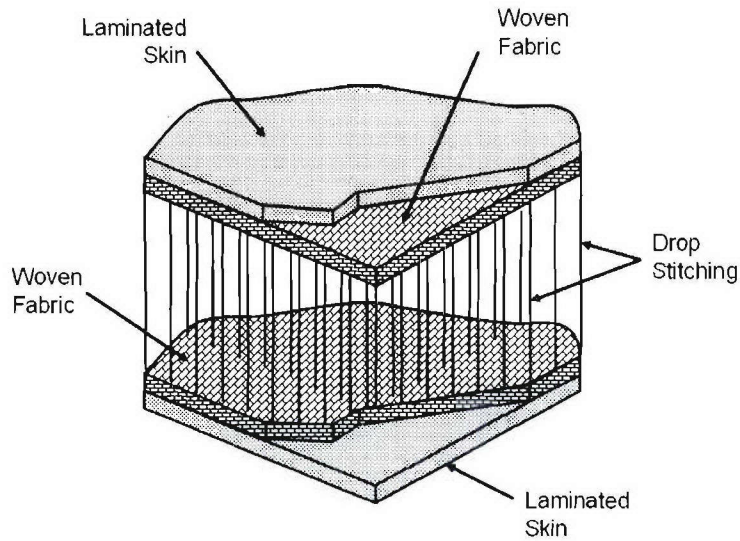

Figure 13. Section view of an example drop-stitch construction for air-inflated fabrics.

EFFECTS OF AIR COMPRESSIBILITY ON STRUCTURAL STIFFNESS

The load-deflection response of air-inflated fabric structures may depend upon additional stiffening influences other than the initial inflation pressure. These may include contributions from nonlinearities in the fabric stress-strain behavior, the work done on the air by external loads, and other phenomena. If appreciable changes in pressure or volume occur during loading, as in the case of energy absorbers, work is performed on the air through compressibility, which stiffens the structure. Air compressibility can be modeled from thermodynamic principles in accordance with the Ideal Gas Law shown in equation (7).

$$P'V = mRT\,, \tag{7}$$

where: P' = the absolute pressure
V = volume
m = mass
R = gas constant for air
T = temperature (°K)

For a quasi-static, isothermal process, the work done on the air by compression is:

$$W_{air} = \int_{V_1}^{V_2} P\,dV = \int_{V_1}^{V_2} \frac{mRT}{V}\,dV = mRT \ln \frac{V_2}{V_1}\,. \tag{8}$$

The total energy of the structure, E_{total}, is the work done by all external forces, W_{ext}, which is related to the total strain energy of the fabric, U_f, and W_{air} as shown in the energy balance of equation (8).

$$E_{total} = W_{ext} = U_f + W_{air}. \tag{9}$$

For homogeneous films and membranes, the elastic and shear moduli are readily determined by standardized tests. However, for the case of plain-woven and braided fabrics, the elastic and shear moduli can vary not only with pressure but also with fabric architecture (plain weave, harness weave, braid, yarn densities, etc.), external loads (crimp interchange), and coatings if present. With increasing pressure, slack within the yarns is removed, the yarns begin to straighten (decrimp) and contact between intersecting yarns at the crossover points causes compaction.

EXPERIMENTS ON PLAIN-WOVEN FABRICS

Hearle[3] identified 3 distinct regions of stiffness for tensile loading of a plain-woven fabric as shown in figure (14). For safe practice, air-inflated fabric structures are designed to operate with yarn forces ranging between regions I and II.

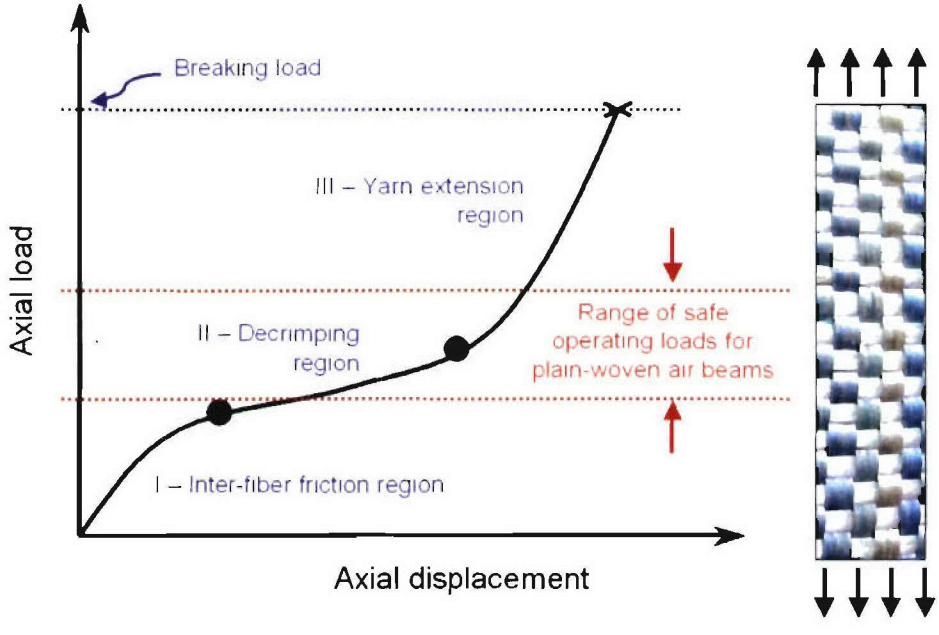

Figure 14. Stages of axial stiffness for woven fabric subjected to tension.

This ensures that the yarns are loaded well below their breaking strengths to provide sufficient factors of safety against burst. Once the fabric is biaxially stressed and subjected to an in-plane shear stress, the yarns will shear (rotate) with respect to their original orientations. The shear stiffness (i.e.; resistance to yarn rotations) results from inter-yarn friction and compaction at the

crossover points. Hence, the shear modulus is actually a system property rather than a constitutive (i.e.; material) property. As the shear rotations increase, an upper bound is reached when yarns of both directions become kinematically locked resulting in what is referred to as shear-jamming. For pure shear loading, the trellising fixture shown in figure (15) can be used. Figure (16) shows the shear force versus shear angle plot of an uncoated Vectran fabric. Further shear loading induces localized shear wrinkling instabilities that lead to increased out-of plane deformations.

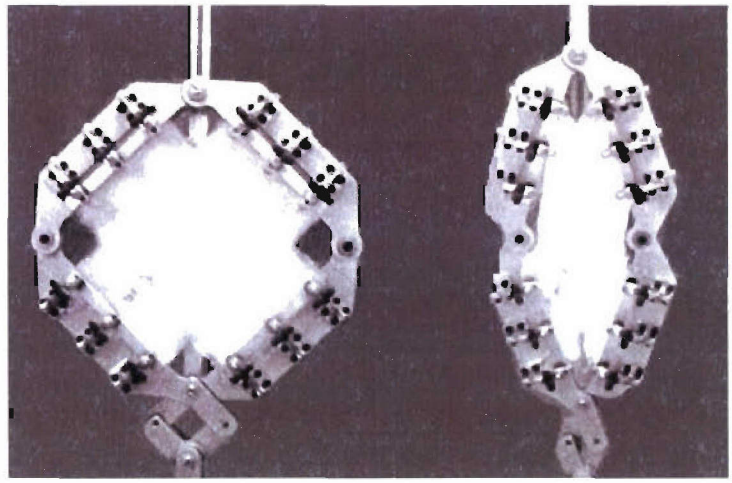

Figure 15. Picture frame test fixture for pure shear loading of fabrics.

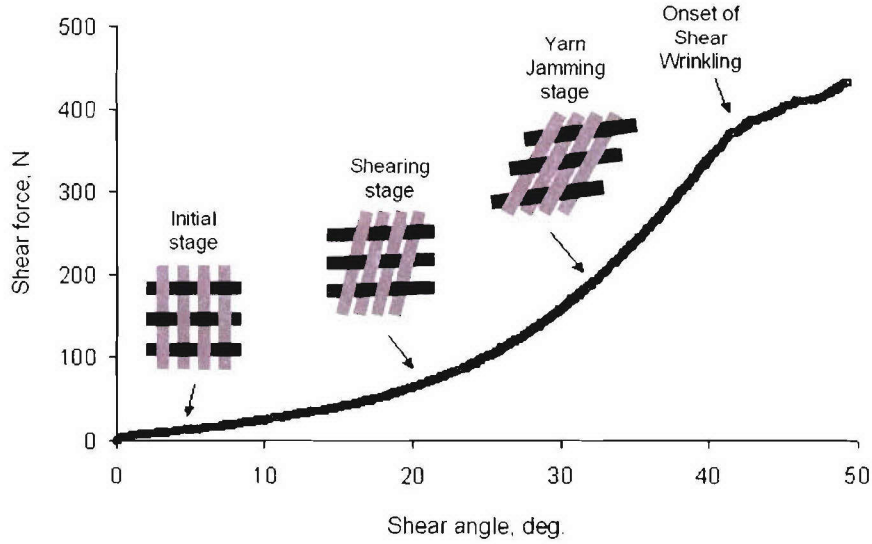

Figure 16. Stages of shear stiffness for pure shear loading of a 2:1 Yarn Density Ratio woven fabric.

Farboodmanesh et al[15] conducted shear tests on rubber-coated, plain-woven fabrics and established that the initial shear response was dominated by the coating and with increased shearing, the behavior of a coated fabric transitions to that of an uncoated fabric.

Unlike fabric structures, the homogeneity of membranes excludes the kinematic motions associated with crimp interchange and strain energy is developed throughout all stages of biaxial tensile loading. However, membrane structures composed of homogenous materials are also susceptible to both bending and shear wrinkling instabilities.

Many testing methods have been developed for evaluating the mechanical properties of yarns and fabrics including ASTM standards, Kawabata Evaluation System, military specifications (MIL-Spec), British standards, etc. It is recommended that the structural engineer become familiar with the applicability of these standards to the design and testing of fabric materials as applicable to air-inflated fabric structures. Saville[16] provides a description of many standard tests used in evaluating fiber, yarns and fabrics.

A recently developed multi-axial tension and shear test fixture[13] was developed to permit simultaneous measuring of E_{warp}, E_{weft} and G_f for structural fabrics. The fixture, as shown in figure (17), was designed for use with conventional tension/torsion machines to characterize the elastic and shear moduli of fabrics as functions of biaxial loads. It utilizes a cruciform-shaped specimen and was designed to evaluate both strength and stiffness properties of various fabric architectures such as weaves, braids and knits subjected to biaxial loads, shear loads or combined biaxial and shear loads. For fabrics constructed of 2 principal fiber directions, the fixture utilizes 2 rhombus-shaped frames connected with rotary joints as shown in figure (17) with the biaxial tension and shear modes illustrated for a plain-woven fabric. For triaxial braided fabrics, the fixture uses a third rhombus-shaped frame with additional rotary joints.

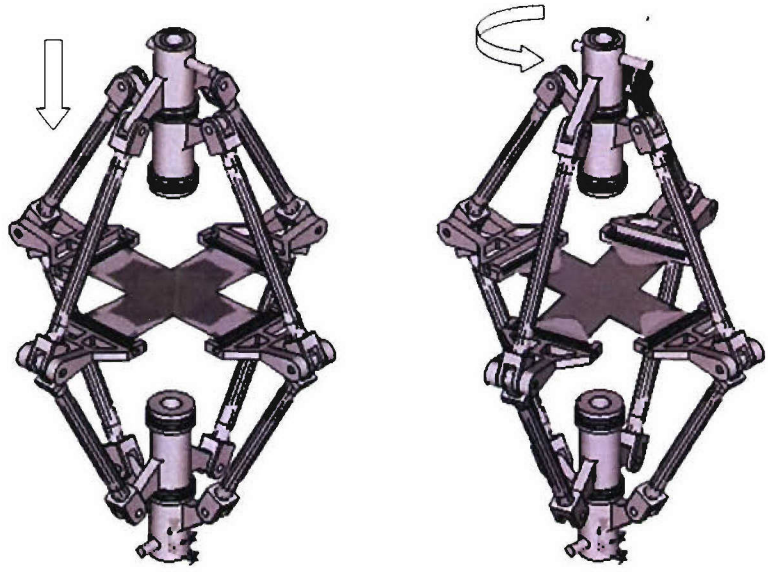

Biaxial tension mode In-plane shear mode

Figure 17. Combined biaxial tension and in-plane shear test fixture. (U.S. Patent No. 6,860,156)

A STRAIN ENERGY-BASED DEFLECTION SOLUTION FOR BENDING OF AIR BEAMS WITH SHEAR DEFORMATIONS

The air beam bending experiments exhibited that, unlike metallic structures, deflections are functions of internal pressure and transverse shear deformations may be significant. If shearing deformations become appreciable, they will increase the total deflection of air-inflated fabric structures. Therefore, a shear-deformable theory such as that developed by Timoshenko[17] must be employed in place of Euler-Bernoulli[18] theory to compute air beam deflections.

This section simulates the 4-point bending experiments and analytically estimates the fabric shear modulus when changes in pressure and volume are negligible. Fabric shearing deformations, which were evident for each of the 4-point bending tests shown in figures (10-12), were observed to decrease with increasing pressure. It will be shown that the shear modulus of the fabric is not a function of the warp yarn's elastic modulus. This was accomplished by deriving a shear-deformable air beam deflection equation for the 4-point loading arrangement described by figure (18). From that equation, and using experimentally obtained air beam deflections, the fabric shear modulus, G_f, can be computed. This equation captured both the bending and transverse shear deformations that comprise the total mid-span deflection.

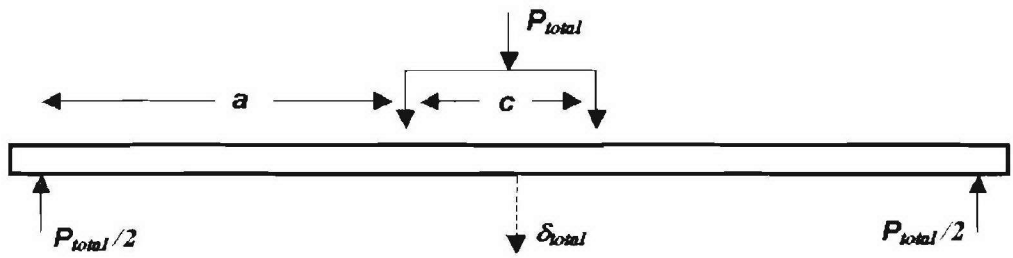

Figure 18. 4-Point bending arrangement for shear deformable beam deflection equation.

The nearly-orthogonal yarn directions were assumed to be truly orthogonal, with the warp axis being parallel to the longitudinal axis of the air beam. This uncoupled the bending stresses from the weft (hoop) yarns. The warp yarns were assumed to exclusively support the bending stresses. In a truly orthogonal fabric air beam, the weft yarns can be considered as parallel rings rather than continuously spiraled yarns with small lead angles. Second, an equivalent cylinder having a cross sectional area equal to the total cross sectional areas of all the warp yarns, A_{total}, was used to represent the actual air beam. The inner radius of the equivalent cylinder, r_i, was taken as the nominal air beam radius and the outer radius of the equivalent cylinder, r_o, was computed by:

$$r_o = \sqrt{\frac{A_{total}}{\pi} + r_i^2} \quad . \tag{10}$$

Castigliano's Second Theorem[18] was used and considered the strain energies from both bending and shearing for the equivalent cylinder. The total strain energy, U_{total}, was expressed as the sum of the bending and shearing strain energies:

$$U_{total} = \int_0^L \frac{M(x)^2}{2E_f I_{cyl}}\,dx + \int_0^L FS\,\frac{V(x)^2}{2A_{cyl}G_f}\,dx \tag{11}$$

where: A_{cyl} = cross sectional area of equivalent cylinder (equal to total area of warp yarns, A_{total})
E_f = fabric elastic modulus along warp (longitudinal) axis measured from biaxial tests
FS = shear strain correction factor (for tube = 2.0)
G_f = pressure-dependent fabric shear modulus
I_{cyl} = area moment of inertia of the equivalent cylinder about bending axis
L = length of air beam
$M(x)$ = bending moment
$V(x)$= transverse shear force along longitudinal axis
x = longitudinal position along air beam.

For thin-walled cylinders of outer radius r_o, and thickness, t_{cyl}, I_{cyl} is computed as shown in equation (10) by neglecting terms containing higher-ordered forms of t_{cyl}.

$$I_{cyl} = \pi r_o^3 t_{cyl}. \tag{12}$$

The total mid-span deflection, δ_{total}, due to the total applied, P_{total}, is derived from minimizing the total strain energy, U_{total}. This leads to:

$$\delta_{total} = \frac{1}{48}\,\frac{8a^3 P_{total} + 12\,c\,a^2 P_{total} + 3c^2 a P_{total}}{E_f I_{cyl}} + \frac{1}{4} FS\,\frac{2\,a\,P_{total}}{G_f A_{cyl}} \tag{13}$$

where: a = distance between support point and adjacent load point
c = distance between load points.

The first and second terms of equation (13) represent the bending component, δ_{bend}, and the shearing component, δ_{shear}, of the total mid-span deflection, respectively. The fabric elastic modulus, E_f, is measured from biaxial tension tests performed on the fabric using the 2:1 weft-to-warp loading ratio. The magnitudes of the warp yarn tension used in the biaxial tests must match the warp yarn forces of the air beam at the inflation pressure of interest. Using the second term, δ_{shear}, the fabric shear modulus, G_f, may be calculated from:

$$G_f = \frac{a P_{total} FS}{2\delta_{shear} A_{cyl}}. \tag{14}$$

Equation (14) indicates that G_f is not a function of the fabric elastic modulus, E_f whereas P_{total} and δ_{shear} are functions of inflation pressure. Alternatively, by determining the shear-jamming angle of the fabric and the corresponding δ_{shear}, a lower bound value of G_f can be determined.

ANALYTICAL & NUMERICAL MODELS

A variety of analytical and numerical models have been developed to predict the load-deflection behavior for inflatable structures[4,13,19-26] and for the load-extension behavior of fabrics themselves[27,28].

UNIT CELL NUMERICAL MODELS

One could create a finite element model of an air beam with all its discrete yarns, bladder, contact surfaces, friction etc., however, research has shown that solutions to such a model would exceed the computational limits of today's hardware. The need to obtain a computationally efficient model that would not exceed hardware limits or encounter convergence problems led to the development of localized yarn interaction models for plain-woven fabrics. These models are commonly referred to as unit cell models.

Unit cell models are used to develop the constitutive behavior on the material scale rather than the structural scale. All sources of influence on constitutive behavior are present on the material scale. Once this behavior is known, it can be applied to the structural scale by using homogenization methods. Homogenization methods simply employ the as-established constitutive behavior from the unit cell models in global structural models constructed of homogenous membranes. This 2-step approach reduces the necessary computations and run time for full-structure modeling while preserving the effects of yarn interactions on material behavior.

A unit cell of a plain-woven fabric generally consists of several rows of warp and weft yarns. Since the yarns exhibit relative displacements and rotations with respect to each other, researchers have investigated two options for treating yarn kinematics: a) rotation-only (pinned centers at the yarn crossover points), and b) rotation and translation at the yarn crossover points as shown in figure (19). In the rotation-only condition, the centers of the contact areas are hinged and remain coincident. Friction is due only to the relative rotation of the yarns and no sliding is allowed. This kinematic condition is appropriate for modeling pneumatic muscles[29] where the fabric is braided and the relative angle of rotation at the yarn crossover points is significantly large. In the rotation and translation condition, no kinematic constraints are imposed at the yarn crossover points. This enables interacting yarns to slide and rotate with respect to each other. Therefore, contact-induced friction forces at the yarn crossover points provide resistance to both relative rotations and translations.

The bladder generally does not contribute any structural stiffness to the fabric nor is it necessary to include the bladder as a contacting media. In addition, the inclusion of a bladder contact surface was found to create unnecessary convergence difficulties and added computational expenses. Since the bladder was eliminated from these models, the unit cell should be subjected to a uniform pressure representing the air-beam pressure. There are several

methods of applying the internal pressure to the unit cell model, depending on the individual preferences.

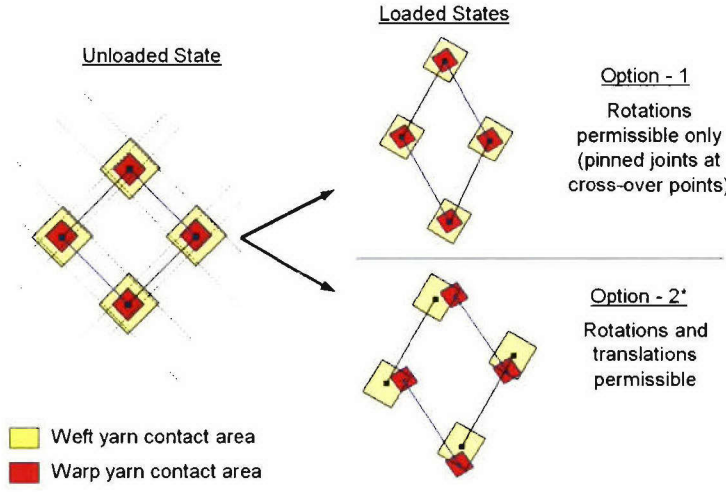

Figure 19. Treatment of yarn kinematics in unit cell models.

Example of a Unit Cell Model

In a specific example of the unit cell, each yarn was represented by an isotropic thin shell with material properties of either Vectran or PEN, depending on the fabric being studied. The shell unit cell model consisted of 4 warp yarns and 4 weft yarns as shown in figure (20). The model was subjected to internal pressures ranging from 0.0138 MPa (1 psi) to 0.276 MPa (20 psi). Contact surfaces were permitted to allow yarn translation and rotations as described by option-2. Two compliant membrane elements ($E_{membrane} << E_{yarn}$) connecting the center points of the contact regions were created. These membrane elements were used to determine the overall stress and strain of the shell unit cell model and did not contribute to the structural stiffness of the model.

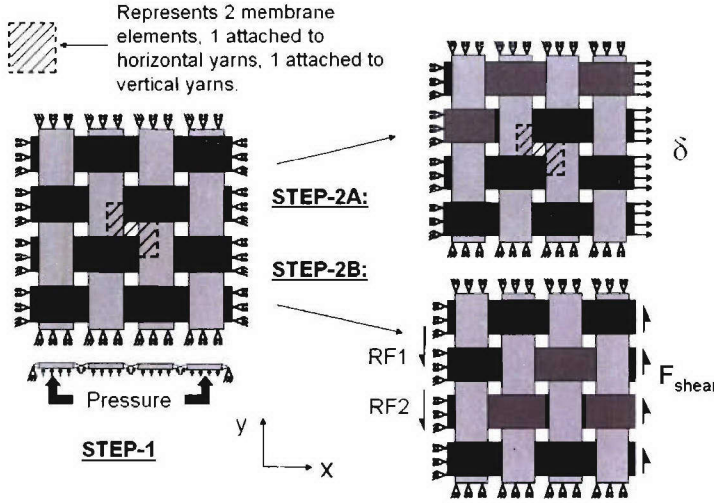

Figure 20. Example unit cell model and loading procedure.

A 3-step computational procedure was employed to determine the elastic and shear moduli of the unit cell. First, the vertical yarns were restrained and the horizontal yarns (x-direction) were subjected to +1% displacement. The model was solved and the stress in the x-direction and the strains in the x- and y-directions were determined. Then, the elastic modulus, $E_1 = \sigma_1/\varepsilon_1$, and Poisson's ratio, $\nu_{12} = -\varepsilon_2/\varepsilon_1$, were determined. Second, the horizontal yarns were restrained and the vertical yarns (y-direction) were subjected to +1% displacement in the y-direction. The model was solved and the stress in the y-direction and the strains in the x- and y-directions were determined. Then, the elastic modulus, $E_2 = \sigma_2/\varepsilon_2$, and Poisson's ratio, $\nu_{21} = -\varepsilon_1/\varepsilon_2$, were determined. Finally, the third step was to calculate the shear modulus. This is difficult due to the fact that the elastic and shear moduli of a plain-woven fabric structure are highly dependent on the internal pressure and, furthermore, the elastic and shear moduli are independent. Two methods are suggested. The first method is for the case where the fabric is coated and there is no relative motion between the yarns, then the following approach is recommended.

Continuum Approach

In this approach the fabric is assumed to be a continuum with orthotropic material properties. The unit cell model in this case was subjected to a +1% nodal displacement at a 45° angle (not shown). The model was solved and the stresses and strains of the unit cell at the 45° angle were determined. The shear modulus was calculated according to Jones[7] by:

$$G_f = \left(\frac{4}{E_x} - \frac{1}{E_1} - \frac{1}{E_2} + \frac{2\upsilon_{12}}{E_1} \right)^{-1} \tag{15}$$

where E_x is the elastic modulus in the direction of the 45° load. This expression may be appropriate for fabrics with stiff coatings.

Non-Continuum Approach

The second approach of calculating G_f assumes that the woven fabric is not a continuum and that each yarn independently responds to the external load. In this case, the horizontal yarns were subjected to a shear force F_{shear}. The shear modulus was then calculated based on the equilibrium of the horizontal yarn and its shear deformation as:

$$G_f = G_{12} = \frac{\tau}{\gamma} \tag{16}$$

where: $\tau_{shear} = \Sigma F_{reaction} / \Sigma A$; and $\gamma = arctan\ (\delta_{shear} / L)$, and where $\Sigma F_{reaction}$ is the sum of reaction forces at the support, δ_{shear} is the nodal transverse displacement, A is the yarn cross section and L is the yarn length.

It is recommended that a number of tests on the unit cell model be performed in which the coefficient of friction is varied and the changes in the elastic and shear moduli are determined. Therefore, the results of the shell unit cell model will be parametric in both friction and pressure.

Structural Air Beam Models

Once the elastic and shear moduli of the membrane elements are determined from the unit cell model, a global structural finite element model of the air beam, using membrane elements, can be created such as the one shown in figure (21). Here, the fabric skin would be discretized using membrane elements. However, nine elastic material constants *(E_1, E_2, E_3, ν_{12}, ν_{13}, ν_{23}, G_{12}, G_{13}, and G_{23})* are required, of which, only E_1, E_2, and G_{12} had been calculated from the beam unit cell model. Because a membrane formulation is used for the fabric skin, the elastic modulus E_3 would not influence the global beam deflection and was therefore chosen to be of the same order of magnitude as E_1 and E_2 (in the order of E_3 = 64,000 MPa for the current example). It was also noted that any load applied in the direction of one yarn is decoupled from all orthogonal yarns. That is, the Poisson's ratio is nearly 0, therefore, the condition that $\nu_{12} = \nu_{13} = \nu_{23} = 0.0$ may be applied. No method was developed to determine G_{13} and G_{23}. It is hypothesized that neither value had a significant effect on the beam deflection. One could examine this hypothesis by a parametric study of values for G_{13} and G_{23}.

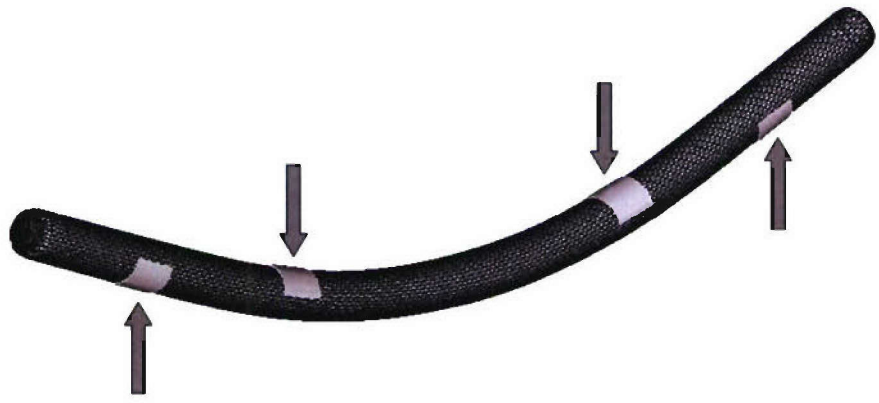

Figure 21. Example of an air beam global finite element model subjected to 4-point bending.

In the abovementioned example, using the analytical strain energy solution, the equivalent in-plane fabric shear modulus, G_f, for the 50.8 mm (2.0 in) diameter Vectran beam pressurized to 0.689 MPa (100 psi) was calculated as 86.06 MPa. (12,480 psi). The computed bending and shear components of the mid-span deflection were 12.39 mm (0.488 in) and 39.54 mm (1.557 in), respectively. The elastic and shear moduli in the beam unit cell model were calculated for an internal pressure of 0.137 MPa (20 psi) as E_1 = 64,033 MPa, E_2 = 64,098 MPa and $G_f = G_{12}$ = 60.96 MPa. Similarly, for an internal pressure of 0.207 MPa (30 psi), the elastic moduli were calculated as E_1 = 64,045 MPa, E_2 = 64,049 MPa and $G_f = G_{12}$ = 80.64 MPa.

CONCLUDING REMARKS

The unit cell modeling method was used to determine the influence of pressure, weave architecture (including yarn density ratio), crimp interchange, coefficients of friction and biaxial loading ratios on the effective fabric elastic and shear moduli. These moduli were shown to increase with increasing pressure. The coefficient of friction between yarns did not influence the elastic and shear moduli significantly because the relative displacements of the interacting yarns were small compared to their cross sections. The shear modulus of plain-woven fabrics was shown to be a system property; it is a kinematic property of the yarn assemblage in fabric form and is independent of the yarn elastic moduli. The use of yarns with higher elastic modulus may not significantly influence the deflection of air beams because crimp interchange can prevent the as-woven yarns from developing their elastic behavior. It has also been shown that coatings can stiffen the fabric material resulting in smaller air beam deflections.

Homogenization is particularly suitable for developing computationally efficient global models of air-inflated fabric structures in conjunction with unit cell methods. The unit cell method captures the nonlinear constitutive behavior of the plain-woven fabric in response to applied loads. This behavior is transferred to a homogeneous material in a global model of the air-inflated fabric structure.

The studies have shown that that air-inflated fabric structures differ fundamentally from conventional metal structures and fiber/matrix composite structures. While the plain-woven fabric may appear to be an orthotropic material, its mechanical behavior indicated otherwise. It does not behave as a continuum, but rather as a discrete yarn assembly.

REFERENCES

1. Celanese Acetate LLC, *"Complete Textile Glossary,"* 2001.
2. Hearle, J.W.S., *"High Performance Fibres,"* Woodhead Publishing, 2001.
3. Hearle, J.W.S., Grosberg, P., Backer, S., *"Structural Mechanics of Fibers, Yarns and Fabrics,"* John Wiley & Sons, Inc., New York, 1969.
4. Cavallaro, P.V., Johnson, M.E., Sadegh, A.M., *"Mechanics of Plain-Woven Fabrics for Inflated Structures,"* Composite Structures Journal, Vol. 61, pp. 375-393, 2003.
5. Pierce, F. T., J. Textile Institute, Vol. 28, T45, 1937.
6. Fung, W., *"Coated and Laminated Textiles,"* Woodhead Publishing, 2002.
7. Jones, R.M., *"Mechanics of Composite Materials,"* Hemisphere Publishing Co., 1975.
8. Cadogan; D.P., Scarborough, S.E., Lin, J.K.H., Sapna III,G.H., *"Shape Memory Composite Development for Use in Gossamer Space Inflatable Structures,"* American Institute of Aeronautics and Astronautics, AIAA 2002-1372.
9. U.S. Patent No. 6,910,308 by Cadogan; D.P., Scarborough, S.E., Lin, J.K.H., Sapna III,G.H.
10. U.S. Patent No. 5,677,023 by Brown, G.
11. U.S. Patent No. 5,735,083 by Brown, G., Sharpless, G.
12. U.S. Patent No. 5,421,128 by Brown, G., Sharpless, G.

13. Cavallaro, P.V., Quigley, C.J., Johnson, A.R., Sadegh, A.M., *"Effects of Coupled Biaxial Tension and Shear Stresses on Decrimping Behavior in Pressurized Woven Fabrics,"* 2004 ASME International Mechanical Engineering Congress and Exposition, Anaheim, CA, November 13, 2004, IMECE2004-59848.
14. Army Center of Excellence for Inflatable Composite Structures, http://nsc.natick.army.mil/media/fact/facilities/ICS.htm
15. Farboodmanesh, S., Chen, J., Mead, J. L., White, K., *"Effect of Construction on Mechanical Behavior of Fabric Reinforced Rubber,"* Rubber Division Meeting, American Chemical Society, Pittsburgh, PA, 8-11 October 2002.
16. Saville, B.P., *"Physical Testing of Textiles,"* Woodhead Publishing, 1999.
17. Timoshenko, S., *"Strength of Materials,"* D. Van Nostrand Company, Inc., 1946.
18. Ugural, A.C., Fenster, S.K., *"Advanced Strength and Applied Elasticity,"* 2nd ed., Elsevier North-Holland Publishing Company, New York, 1977.
19. Bulson, P. S., *"Design Principles of Pneumatic Structures,"* The Structural Engineer, Vol. 51, No. 6, June 1973.
20. E Steeves, E.C., *"Fabrication and Testing of Pressurized Rib Tents,"* Technical Report 79-008, United States Army, Soldier Biological Chemical Command, Natick, MA, 1979.
21. Steeves, E.C., *"The Structural Behavior of Pressure Stabilized Arches,"* Technical Report 78/018 (AD-A063263), United States Army, Soldier Biological Chemical Command, Natick, MA, 1978.
22. Steeves, E.C., *"Behavior of Pressure Stabilized Beams Under Load,"* Technical Report 75-47-AMEL, United States Army, Soldier Biological Chemical Command, Natick, MA, 1975.
23. Steeves, E.C., *"A Linear Analysis of the Deformation of Pressure Stabilized Beams,"* Technical Report AND-006-493, United States Army, Soldier Biological Chemical Command, Natick, MA, 1975.
24. Steeves, E.C., *"Pressure Stabilized Beam Finite Element,"* Technical Report 79-002, United States Army, Soldier Biological Chemical Command, Natick, MA, 1978.
25. W. B. Fichter, *"A Theory for Inflated Thin-Wall Cylindrical Beams,"* NASA Technical Note D-3466, National Aeronautics and Space Administration, Washington, DC, 1966.
26. Stein, M., Hedgepeth, J.M., *"Analysis of Partly Wrinkled Membranes,"* Technical Note D-813, NASA Langley Research Center, July 1961.
27. Freeston, W. D., Platt, M. M., Schoppee, M. M., *"Mechanics of Elastic Performance of Textile Materials, Part XVIII, Stress-Strain Response of Fabrics Under Two-Dimensional Loading,"* Textile Research Journal, Vol. 37, pp 948-975, 1967.
28. Sidhu, R. M. J. S. R., Averill, C., Riaz, M., Pourboghart, F., *"Finite Element Analysis of Textile Composite Preform Stamping,"* Journal of Composite Structures, vol. 52, 2001, pp. 483-497.
29. K. G. Klute and B. Hannaford, *"Finite Element Modeling of McKibben Artificial Muscle Actuators,"* IEEE/ASME Transactions on Mechatronics, March 1998.

REPORT DOCUMENTATION PAGE

Form Approved
OMB No. 0704-0188

1. AGENCY USE ONLY *(Leave blank)*	2. REPORT DATE	3. REPORT TYPE AND DATES COVERED
	5 November 2006	

4. TITLE AND SUBTITLE

AIR-INFLATED FABRIC STRUCTURES

5. FUNDING NUMBERS

6. AUTHOR(S)

Paul V. Cavallaro
Ali M. Sadegh

7. PERFORMING ORGANIZATION NAME(S) AND ADDRESS(ES)

Naval Undersea Warfare Center Division
1176 Howell Street
Newport, RI 02841-1708

8. PERFORMING ORGANIZATION REPORT NUMBER

RR 11,774

9. SPONSORING/MONITORING AGENCY NAME(S) AND ADDRESS(ES)

10. SPONSORING/MONITORING AGENCY REPORT NUMBER

11. SUPPLEMENTARY NOTES

Reprint of a chapter in *Marks' Standard Handbook for Mechanical Engineers*, Eleventh Edition, McGraw-Hill, New York, 2006.

12a. DISTRIBUTION/AVAILABILITY STATEMENT

Approved for public release; distribution is unlimited.

12b. DISTRIBUTION CODE

13. ABSTRACT (Maximum 200 words)

Air-inflated fabric structures fall within the category of tensioned structures and provide unique advantages in their use over traditional structures. These advantages include light weight designs, rapid and self-erecting deployment, enhanced mobility, large deployed-to-packaged volume ratios, fail-safe collapse, and possible rigidification.

Most of the research and development pursued in air-inflated structures can be traced to space, military, commercial, marine engineering and recreational applications. Examples include air ships, weather balloons, inflatable antennas and radomes, temporary shelters, pneumatic muscles and actuators, inflatable boats, temporary bridging, and energy absorbers such as automotive air bags. However, the advent of today's high performance fibers combined with continuous textile manufacturing processes has produced an emerging interest in air-inflated structures. Air-inflated structures can be designed as viable alternatives to conventional structures.

14. SUBJECT TERMS

Inflated Fabric Structures Air Beams Tension Structures Fiber Kinematics Fabric Mechanics Crimp Interchange Finite Element Analysis Weave Braid Biaxial Testing Drop Stitch Damage Tolerance Fibers Yarns Rigidification Air Compressibility

15. NUMBER OF PAGES
36

16. PRICE CODE

17. SECURITY CLASSIFICATION OF REPORT	18. SECURITY CLASSIFICATION OF THIS PAGE	19. SECURITY CLASSIFICATION OF ABSTRACT	20. LIMITATION OF ABSTRACT
Unclassified	Unclassified	Unclassified	SAR

INITIAL DISTRIBUTION LIST

Addressee	No. of Copies
Defense Technical Information Center	12